COMPUTATIONAL STUDY OF WATER OVER TITANIUM DIOXIDE SURFACES

By

SRINIVAS CHAKRAVARTHY MUSHNOORI

A thesis submitted to the

Graduate School-New Brunswick

Rutgers, The State University of New Jersey

In partial fulfilment of the requirements

For the degree of

Master of Science

Graduate Program in Chemical and Biochemical Engineering

Written under the direction of

Meenakshi Dutt

And approved by

_____

_____

_____

New Brunswick, New Jersey

January 2017

ABSTRACT OF THE THESIS

Computational Study of Water of Titanium Dioxide Surfaces

By: SRINIVAS CHAKRAVARTHY MUSHNOORI

Thesis Director:

Meenakshi Dutt

Given the potential of Titanium Dioxide as a source of alternative energy, drug delivery, protein adsorption, etc. it is imperative that the underlying mechanism of surface-water interactions be thoroughly understood. To this end, our study employs Molecular Dynamics simulations to establish a nanoscale, all atomistic model to capture the mechanistics of the interfacial interactions of water with a Titanium Dioxide surface. Two polymorphs of Titanium Dioxide, Anatase (101) and Rutile (110), are simulated and various aspects of their interfacial behavior studied. Further, a comparison is made between two different electrostatic models, namely, the Multi-Level Summation and the Screened Coulomb potential. The outcome of these studies can guide the adoption of suitable electrostatic potentials for examining bulk-scale behavior in titania-water systems. To this end, a specific case of Titanium Dioxide decorated with Platinum atoms is studied using the Screened Coulomb potential.

ACKNOWLEDGEMENT

I would like to express my most sincere gratitude to my advisor Dr. Meenakshi Dutt for her constant support during my coursework and thesis research and for her patience, insight, and dedication at every step of the way. Beyond the scientific knowledge that I have gained through working under her guidance, I have also learned *how* to think: something that I believe will stand me in good stead lifelong. I would like to thank Dr. Leebyn Chong, who taught me the ropes when I first joined the group, and my labmates Dr. Fikret Aydin, Xiaolei Chu. I extend my gratitude to the committee members, Dr. Masanori Hara and Dr. Tewodros Asefa for their critique of my work. My most sincere thanks go out to the Rutgers Discovery and Informatics Institute (RDI^2) and the eXtreme Science and Engineering Discovery Environment (XSEDE) for providing the computational resources used in this research.

I would also like to thank my friends, Kartheik Iyer, Harini Kantamneni, Malathi Kalyanikar and Yaqoot Shaharyar for helping me with proofreading my writing. Finally, I am extremely thankful to my parents, Padma Mushnoori and Shivkumar Mushnoori for their constant support and my brother Sriharsha Mushnoori for his honest and thoughtful critiques. This thesis could not have been completed without them.

TABLE OF CONTENTS

LIST OF FIGURES

LIST OF TABLES

1. INTRODUCTION

Titanium dioxide has a wide range of potential applications, such as photochemical degradation of organic compounds [1,2,3], protein adsorption[4], and even water splitting for use as a source of alternative energy[5,6,7]. Titanium dioxide has become the most popular (and studied) choice for a variety of applications due to its abundance, low cost, non-toxicity, high chemical and thermal inertia. A central phenomenon in these applications of TiO_2 is its unique interaction with water. While experimental studies on the phenomenon are quite abundant, computational studies, which are important from the standpoint of understanding mechanistic aspects of interface interaction, are quite scarce. These investigations include interfacial interactions between bare titania and water [8, 9, 10], and water-rutile interface dynamics of physically adsorbed water molecules[11].

This study focuses on understanding the structure and dynamical behavior of water molecules over titania surfaces via an all atom representation used in conjunction with the molecular dynamics simulation technique. The study compares anatase (101) and rutile (110) surfaces using the Lennard-Jones and Buckingham potentials to model van der Waals interactions and the Screened Coulomb potential and Ewald Summation to model electrostatic interactions and draws conclusions regarding the comparative accuracy of the different models. Furthermore, the model that employs the screened Coulomb potential is applied to a specific case of Titanium Dioxide in both anatase (101) and rutile (110) forms decorated with Platinum adatoms[28] and studied.

2. METHODS

The system dynamics are resolved by using classical molecular dynamics (MD) simulations[12,13,14]. The equation of motion for each atom i is given by $\mathbf{F}_i = m_i\mathbf{a}_i$ where $\mathbf{F}_i$ is the force acting on atom i, m_i is the mass and $\mathbf{a}_i$ is its acceleration. The force can be expressed as the gradient of the potential energy U by the relation $\mathbf{F}_i = -\nabla_i U$ with $U = U_{VDW} + U_Q$, where U_{VDW} and U_Q are the potential energies arising from van der Waals and electrostatic interactions, respectively. The dynamics of each atom i can be determined by the following equations $-\nabla_i U = m_i\mathbf{a}_i = m_i\frac{\partial^2\mathbf{r}_i}{\partial t^2} = m_i\frac{\partial\mathbf{v}_i}{\partial t}$ and $\mathbf{v}_i = \dot{\mathbf{r}}_i$, where $\mathbf{r}_i$ and $\mathbf{v}_i$ are the position and velocity vectors of atom i. The equations of motion will be integrated using the Velocity Verlet method which has greater stability, time reversibility and preserves the simplectic form in the phase space compared to the Euler method [13,14]. The MD simulations are run using the open source parallelized MD program called LAMMPS [15].

3. THEORY

3.1 Non Bonded Interactions

The interactions between non-bonded atoms are captured by pair potential energies. The van der Waals interactions are modeled as 12-6 Lennard-Jones (LJ) potentials with the functional form[14]

$$E_{LJ} = 4\varepsilon \left[(\sigma/r)^{12} - (\sigma/r)^{6} \right], \quad r < r_c \qquad (1)$$

where the potential cutoff distance r_c is set at 2.5σ for all atom pairs. The electrostatic interactions are captured by the screened Coulombic potential to account for the screening by

$$E_{SC} = (q_i q_j / 4\pi\varepsilon_r r) \exp(-\kappa r) \qquad (2)$$

where ε_r is the relative permittivity or dielectric constant and κ is the inverse Debye length. Since the interface is considered to be aqueous, it is assumed that the electrostatic interactions between the partial charges can be explained by the Debye-Huckel theory [16]. We maintain a relative permittivity of 80 which is equivalent to bulk water and a Debye length of 0.7 nm so that the Coulomb energy is balanced by thermal fluctuations. For validation, we simulate small areas of rutile-water and anatase-water systems to compare results from the screened Coulombic potential with the multilevel summation method (MSM) for electrostatic forces[17].

3.2 Water model

We utilize an extended simple point charge (SPC/E) water model due to its good agreement with bulk properties[18,19]. The water molecule has a bent configuration with a fixed angle of 109.47° and oxygen-hydrogen bond length of 1 Å [19,20]. The partial charges are -0.8476e and 0.4238e for the oxygen and hydrogen

atoms, respectively[19,20]. The effective LJ radius of the water molecule originates from the oxygen center such that σ_{OO} is 3.166 Å and ε_{OO} is 650 J/mol, with no LJ parameters assigned to the hydrogen atoms[20].

3.3 Surface

The rutile (110) and anatase (101) surfaces were constructed using exisiting protocols for TiO_2-H_2O systems via ab initio[21] and density functional theory (DFT) methods[22]. The interaction of TiO_2 with water is captured by the LJ potential with parameters derived from contact angle measurements[23]. Using the combination rules of $\varepsilon_{ij} = (\varepsilon_i\varepsilon_j)^{1/2}$ and $\sigma_{ij} = (\sigma_i+\sigma_j)/2$, the surface-water LJ parameters are ε_{TiO} = 215.128 J/mol and σ_{TiO} = 2.9975 Å. Partial charges for the surface are set to be q_{Ti} = 2.196e and q_O = -1.098e based on the bulk atomic charges[21]. For some of the studies we have used the Buckingham potential; the corresponding parameters are provided in Table 1[21].

Atoms(i-j)	**A_{ij}, kcal mol^{-1}**	**ρ_{ij}, Å**	**C_{ij}, kcal mol^{-1} Å^6**
O-O_{water}	271716.3	0.234	696.8883
Ti-O_{water}	28593.02	0.265	148.000

Table 1: Buckingham potential parameters.

3.4 Simulation setup

We simulate water adsorption on rutile (110) and anatase (101) using a canoncial ensemble with a Langevin thermostat applied to maintain the temperature at 298 K[24]. The total area of TiO_2 surface is at least 316.6 Å x 316.6 Å. The TiO_2 surface supports a layer of water of height 31.66 Å at a density of 1 g/mL. Parallel to the surface and at the height of the water layer is a hydrophobic wall which

accommodates the non-periodic boundaries in the Z dimension. The systems are equilibrated for 4.267 ns and are sampled every 42.67 ps over an interval of 4.267 ns. To ensure reproducibility of results, simulations for each system are repeated using a different random seed.

4. RESULTS AND DISCUSSION

4.1 Bare Titanium Dioxide Surfaces

Publication: A Computational Study of the Organization and Dynamics of Water on Anatase (101) and Rutile (110) Titania Surfaces: The Effect of Electrostatic Models, S. Mushnoori, L.Chong and M. Dutt, 2016, under review.

Collaborators: Leebyn Chong, PhD

Figure 1a and 1b show bare anatase and rutile for a small number of unit cells. Figure 1c shows SPC/E water molecules above the rutile surface.

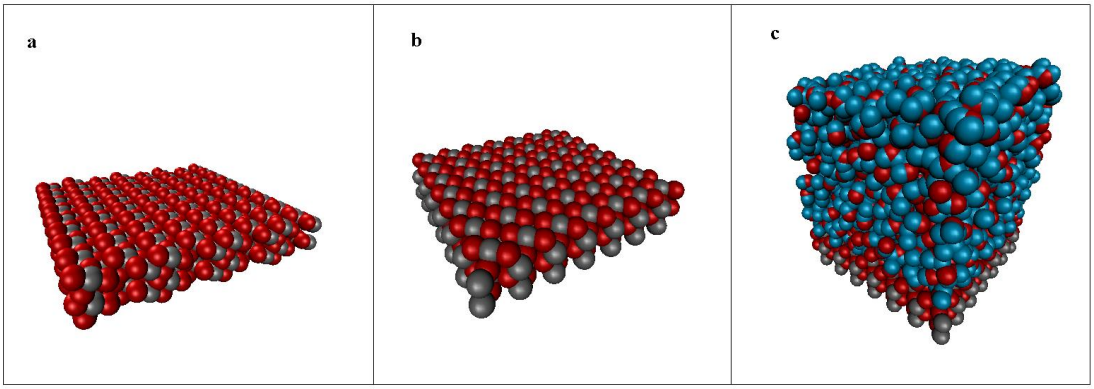

Figure 1: Visualization of (a) anatase (101), (b) rutile (110) where gray is Ti and red is O, and (c) shows a rutile (110) surface with SPC/E water, where cyan is H and red is O.

4.1.1. Diffusion Coefficients

As validation of the model, we examine a dynamic property of water by computing its diffusion coefficient in bulk and near the TiO_2 surface via measurements of the mean squared displacement. Using the unscreened Coulombic potential with long-range MSM solver and dielectric constant of one corresponding to a vacuum medium, we find the self-diffusion coefficient of water in the bulk to be given by 2.950 nm^2/ns which is in good agreement with a value of 2.94 nm^2/ns from other simulation studies[18]. The discrepancy with experimental measurements of diffusion coefficient

of 2.299 nm^2/ns arises due to the assumption of the rigid bonds and angles[25]. When the screened Coulomb Potential is employed, we observe an increase in the diffusion coefficient to 6.217 nm^2/ns. We observe similar results when the screened Coulomb potential is replaced by the MSM solver with a dielectric constant of 80. Table 2 summarizes the average diffusion coefficients for each system and electrostatic model. There is a noticeable decrease in the diffusion coefficient of water for the TiO_2-water system in comparison to the corresponding value for bulk water, with equivalent electrostatic models. We attribute adsorption of water onto the TiO_2 surface to influence the diffusion coefficient as the regular organization of partial charges in the surface results in the short-range ordering of the water molecules.

System	**Electrostatics**	**Dielectric**	**Diffusion Coefficient (nm^2/ns)**
Bulk	MSM	1	2.950
Bulk	MSM	80	6.217
Bulk	Screened	80	5.433
Rutile	MSM	1	1.783
Rutile	MSM	80	5.650
Rutile	Screened	80	4.567
Anatase	MSM	1	2.050
Anatase	MSM	80	4.517
Anatase	Screened	80	4.300

Table 2: Diffusion Coefficients

4.1.2. Radial Distribution Functions

We also validate the model through structural characterization captured by the radial distribution function (RDF) of the water molecules. Our RDF measurements for bulk water agree with results for LJ fluids[26], as shown in Figure 2a. We observe a difference in the organization of water molecules around a given water molecule; the organization is found to depend on the dielectric constant and not the electrostatic model. The first coordination shell, for a dielectric constant of one, is found to lie closer to the reference molecule with more coordinating water molecules than for a dielectric constant of 80. Figures 2b and 2c show similar trends for rutile and anatase, respectively. Our measurement for the RDF of water away from the surface is observed to be similar for rutile and anatase systems, and agrees with RDF measurements for bulk water. We note that the density profile measurements normal to the surface distinguishes the packing of the water molecules due to adsorption on the TiO_2 surface.

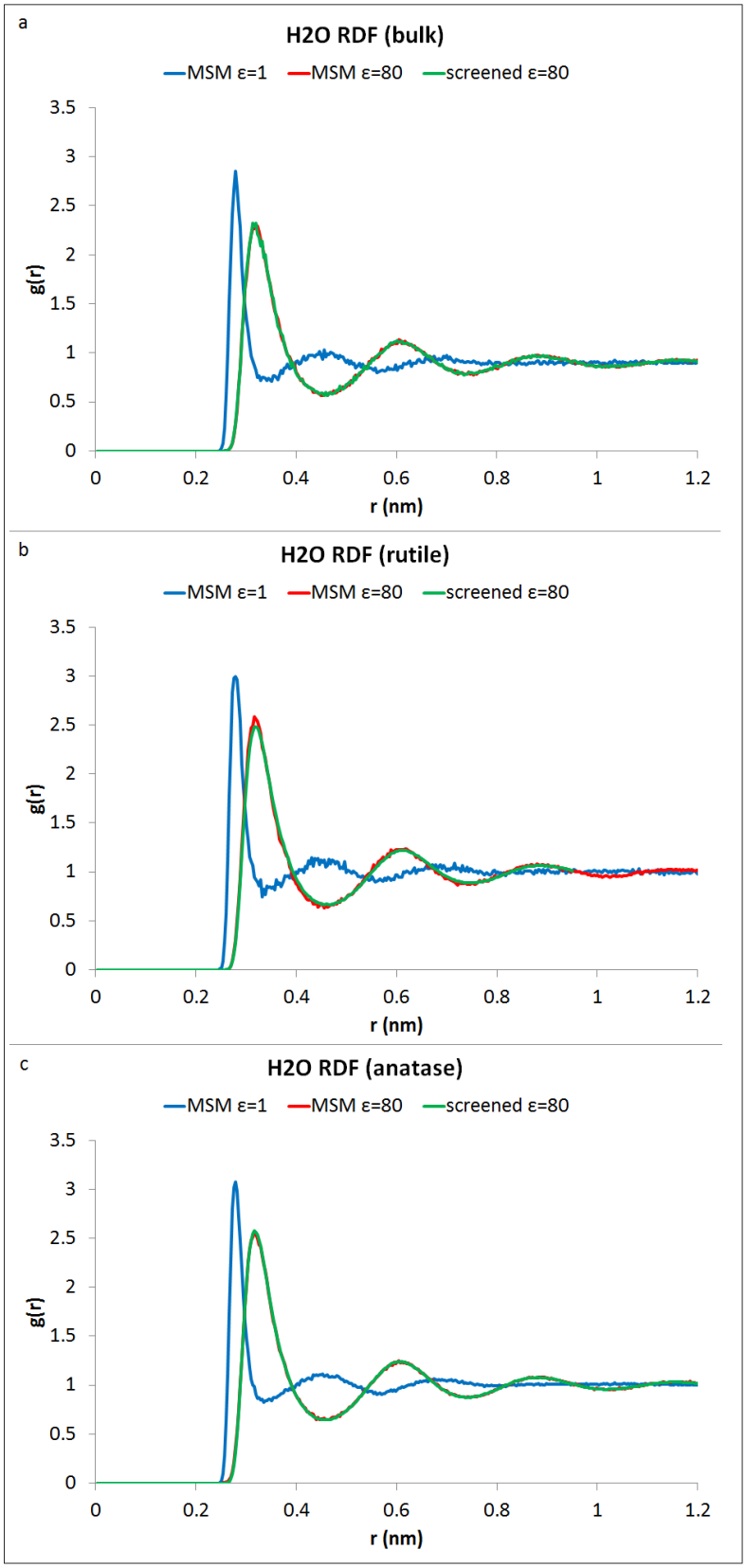

Figure 2: Radial distribution functions for water (a) in bulk, (b) near rutile, and (c) near anatase.

4.1.3. Water dipole angle orientation

We have studied the behavior of water dipoles near the surface by measuring the angles with respect to two different vectors: the surface normal and the pair vector drawn from the surface atom to the center of the water molecule in question (see Figure 3). The angles are defined such that an angle of 180^0 indicates an orientation normal to the surface with the oxygen atom pointing towards the surface, and an angle of 90^0 implies a parallel orientation.

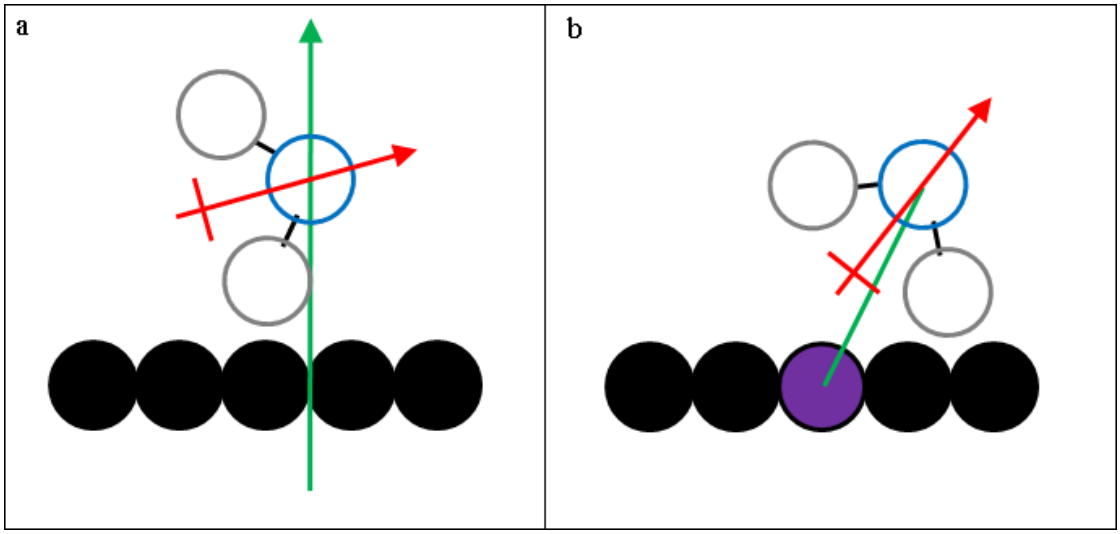

Figure 3: Diagram depicting the angle measurement scheme for (a) a water molecule oriented at an angle to the Z axis (surface normal), and (b) a water molecule oriented at an angle with respect to an axis drawn from a specific reactive site (shown in purple).

The dipole orientation distribution as a function of the angle follows a normal distribution. This occurs because the probability of finding a dipole vector of length r with an orientation θ is directly proportional to the circumference of the circle in a sphere of radius r when the radius vector makes an angle θ with the axis in question

(see Figure 4). Therefore, the angles closer to 90^0 will contribute with greater frequency to the distribution than those close to 0^0 or 180^0. The normal curves can be incorrectly interpreted to suggest that the angles formed tend to cluster around 90^0. A normal distribution represents a completely random orientation of the water dipoles without any preferential alignment. To avoid this artefact, we have normalized the angles to give a uniform distribution of the orientations of the water dipoles. The normalization was done as follows:

$$Distribution = (Angle\ Count) / (N \times Sin\ \theta) \qquad (3)$$

where the angle count is the frequency of vectors oriented at the angle θ and N is the total number of water molecules in the system. Normalization has been done with respect to both N (since two systems do not necessarily have the same number of water molecules) as well as the sine of the angle (to compensate for the frequent contributions from angles close to 90^0). We observe the dipole angle distribution in the bulk water system (for measurements with respect to the z-axis) for the screened Coulombic potential to be uniform, indicating that the water dipoles do not have a preferred orientation. We report similar findings when the screened Coulombic potential is replaced by the MSM solver with a dielectric constant of 1 or 80, and for the anatase and rutile systems with a dielectric constant of 80 (see Figures 4 a-b). However, using the full Coulomb potential with a dielectric constant of 1 and the MSM solver, the preferred orientations are observed to be around 65^0 for both the anatase and rutile systems. Further, in the rutile system there is a second peak that occurs around 177°, which is not observed in the case of anatase (see Figure 4c). This may be attributed to the differences in their respective surface morphologies: in

anatase, the exposed (5-coordinated) titanium atoms are positioned relative to the exposed (2-coordinated) oxygen atoms (as shown in Figure 5b) such that the separation between these oppositely charged centers inhibits an orientation partial to any one of them, preventing a clear peak from being observed. Also, the differences caused by the dielectric constant are subtle. We hypothesize that this is because of the use of the SPC/E model, which effectively treats water molecules as hard spheres once they are within a distance of 0.3166 nm from each other (or other atoms). This constraint inhibits the water molecules from getting sufficiently close to the surface to experience electrostatic interactions with it. To test this hypothesis, we ran simulations under exactly the same conditions but replaced the surface-water LJ interactions with a softer Buckingham Potential to allow the water dipoles to come within sufficiently close proximity to the surface to interact with it. In the anatase system, the sharp peaks occur around 7° and 154°, which indicates that the water molecules adopt orientations with either the oxygen or one of the hydrogen atoms pointing almost directly upwards (see Figure 4d). The rutile system shows similar behavior without the Buckingham potential, but the peak at around 176° is exaggerated (see Figure 4d). Measurement of the distributions for the pair vectors while employing the Screened Coulomb potential and the MSM solver using a dielectric constant of 80 demonstrate uniform distributions. We note in this case that the angles are independent of the solver used; both the MSM solver and screened Coulomb Potential result in identical distributions, as shown in Figure 4e. Using the full Coulomb potential (MSM solver, ε=1), peaks were observed at about 60° and 175° which became exaggerated upon introduction of the Buckingham Potential. The angles measured from the pair vectors are similar for the two surfaces (see Figure 4f).

Differences in the angle distribution between our results and an early study[8] are attributed to the distinction in the water models.

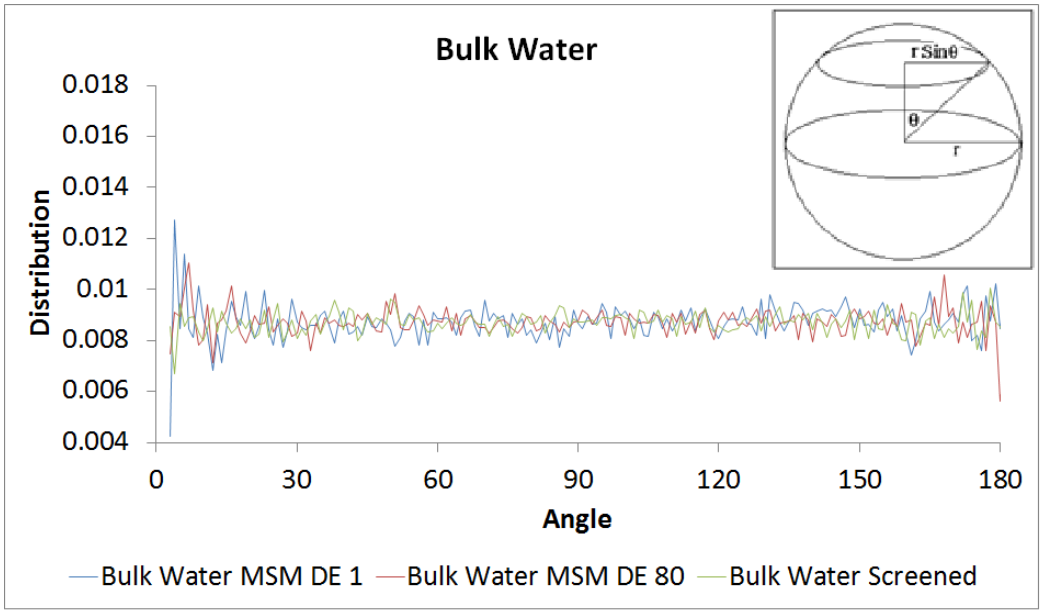

Figure 4a: Angle distributions for bulk water, Inset: Normalization scheme. A vector drawn from the center of a sphere of radius r to its surface at an angle of θ to the normal intersects it at a point on a circle of the sphere with radius rSinθ.

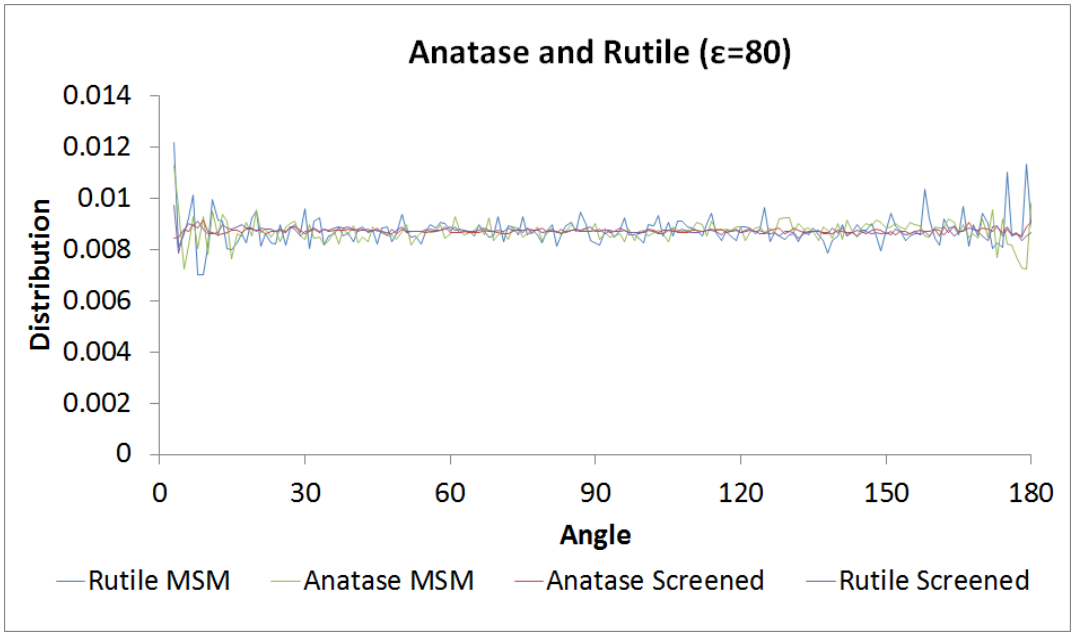

Figure 4b: Angle distributions near Anatase and Rutile surfaces at ε=80.

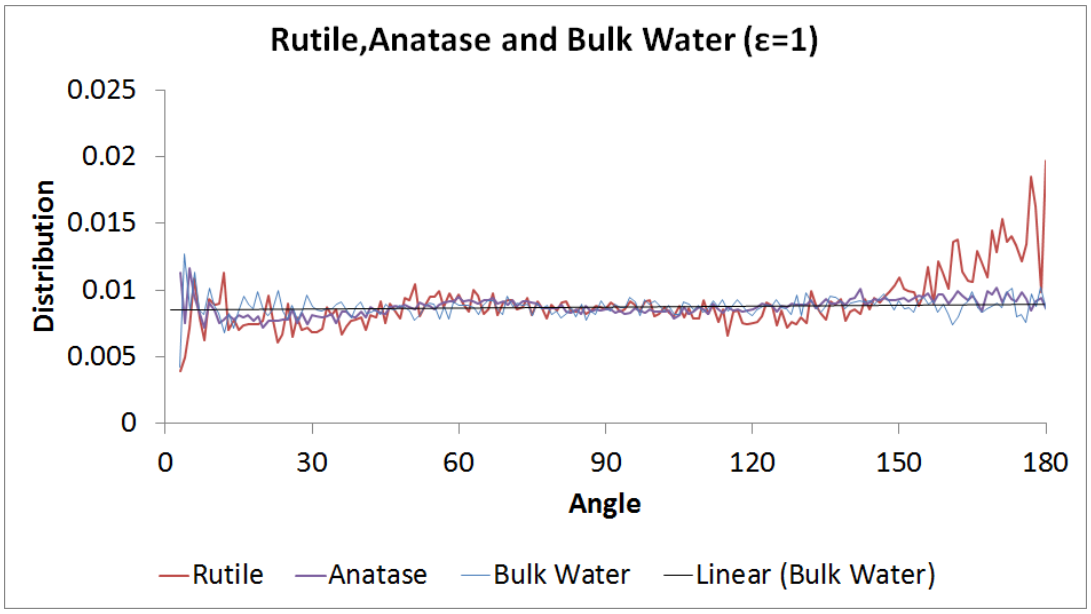

Figure 4c: Angle distributions near Anatase and Rutile surfaces at ε=1.

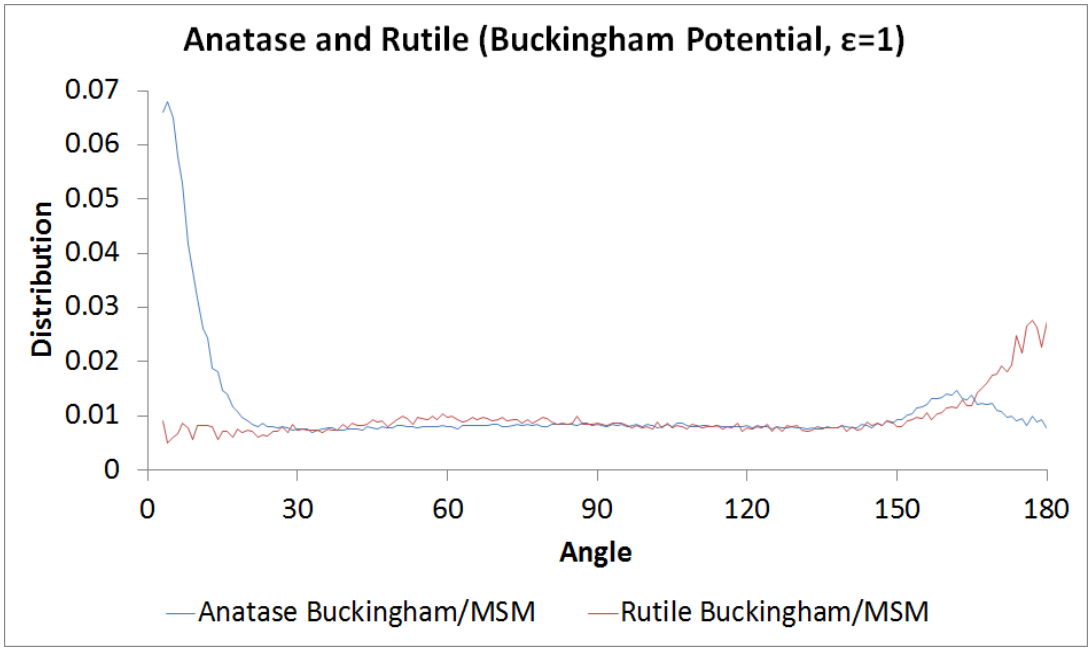

Figure 4d: Angle distributions near Anatase and Rutile surfaces, with Buckingham potential between the fluid and surface at ε=1.

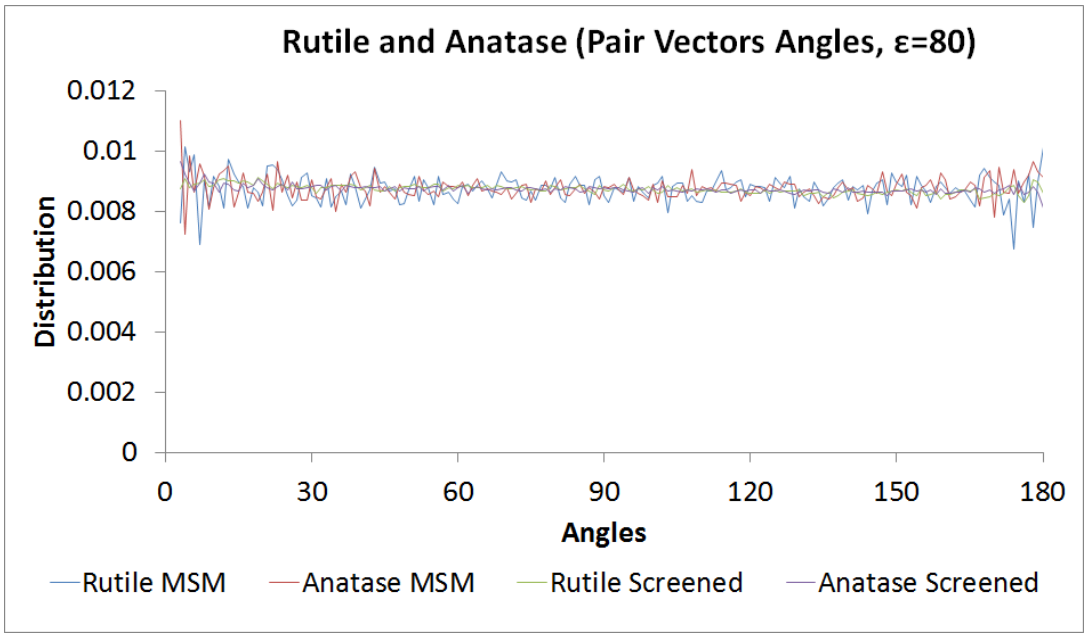

Figure 4e: Angle distributions with respect to pair vectors, ε=80.

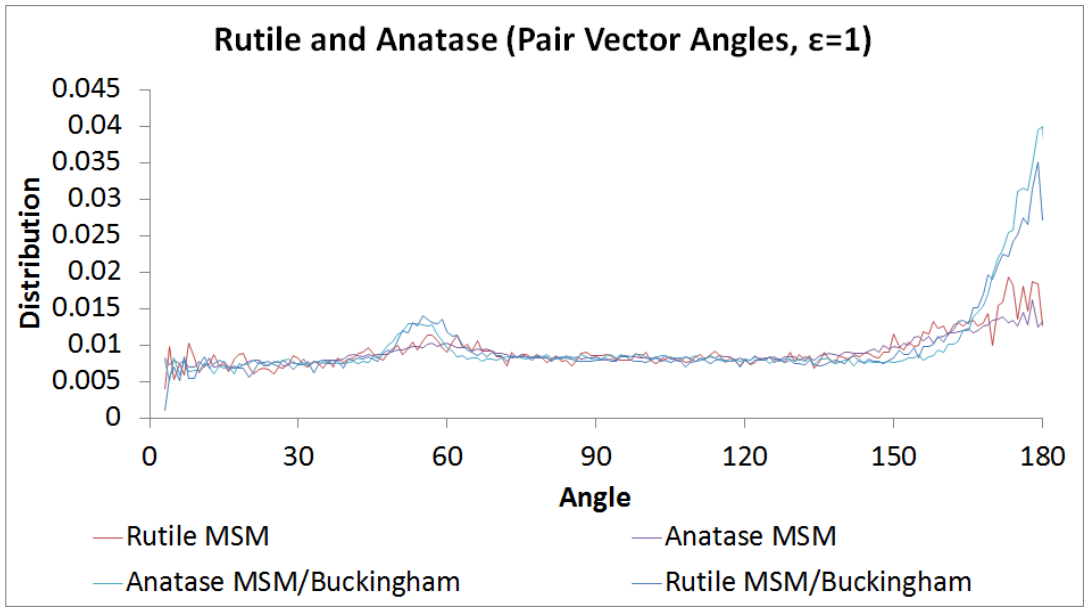

Figure 4f: Angle distributions with respect to pair vectors, ε=1.

4.1.4. Residence Time Distributions

In order to calculate the reaction rates or conversion ratios it is imperative that we understand, as a part of the behavior of water molecules near the catalytic surface, the time spent by a given water molecule in the vicinity of a catalytic active site: a factor that has a direct influence on the water splitting reaction. We have analysed the residence times of the water molecules in the vicinity of a given surface atom. Residence time was defined as the time spent by a water molecule inside a hemisphere of radius 1.5 σ_{OO} from a given surface atom[27]. Residence times have been calculated with respect to (i) oxygen atoms, (ii) titanium atoms, and (iii) all oxygen and titanium surface atoms. In systems where the Screened Coulomb Potential is employed, the water molecules that reside for the longest interval of time in the vicinity of a specific surface atom shows a residence time of roughly 40 ps, after which the distribution drops to a near-zero value (as shown in Figures 5a-b). However, when the MSM solver is used with a dielectric constant of 1, the anatase system shows residence times of 60 ps, with corresponding values of 80ps for the rutile system (see Figures 5c-d). The residence time further increases when the Buckingham potential is used, as shown in Figures 5e-f. These observations are in agreement with our diffusion coefficient measurements. A dielectric constant of 1 results in a smaller diffusion coefficient, causing lower mobility of water molecules and hence, higher residence times. When the Buckingham potential is used, the water molecules are in closer proximity to the surface atoms and have stronger interactions. Hence, the effects of adsorption on the surface become slightly more pronounced, resulting in higher residence times.

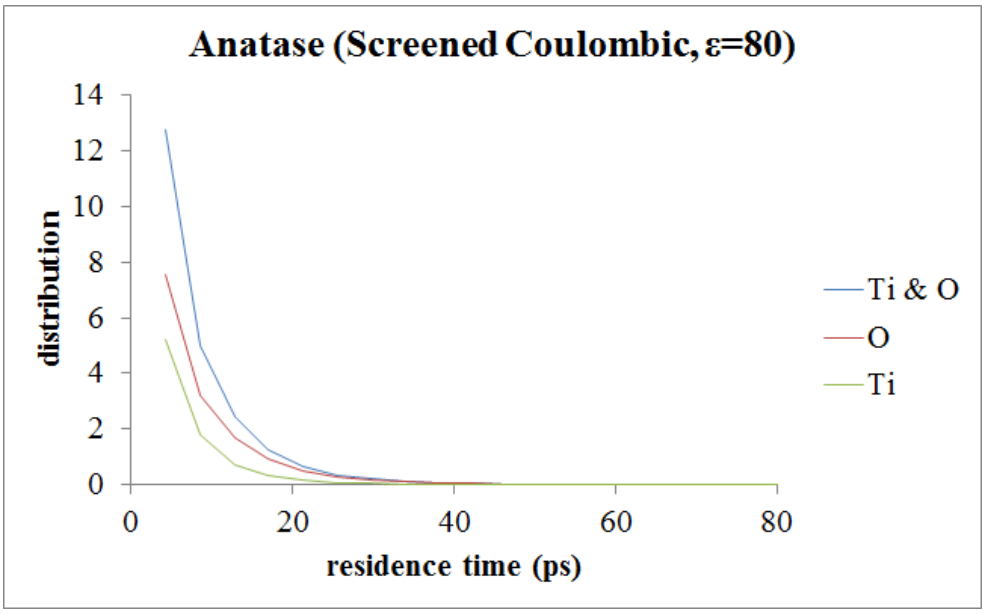

Figure 5a: Residence time distribution of water over Anatase with a dielectric constant of 80.

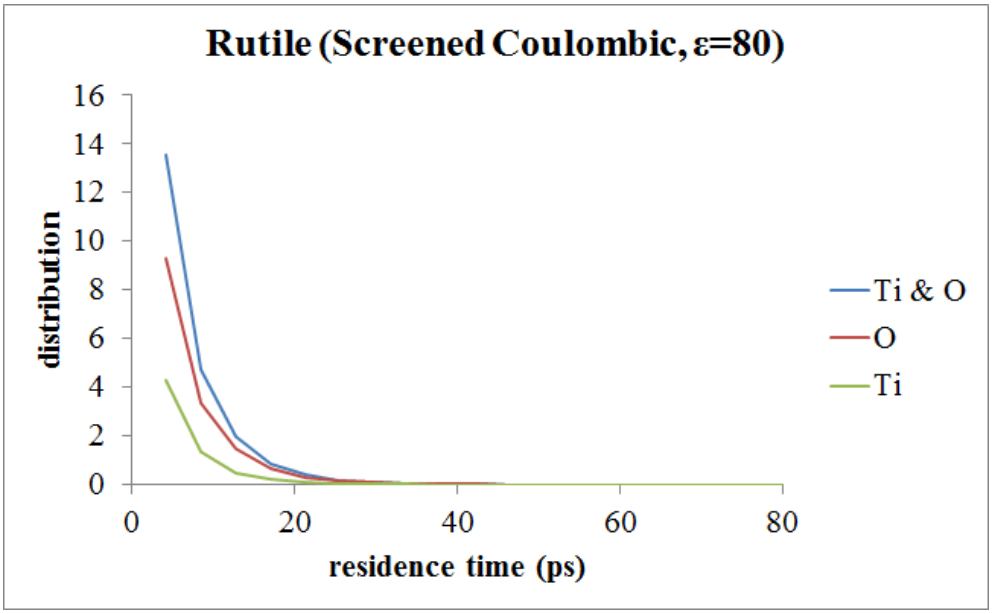

Figure 5b: Residence time distribution of water over Rutile with a dielectric constant of 80.

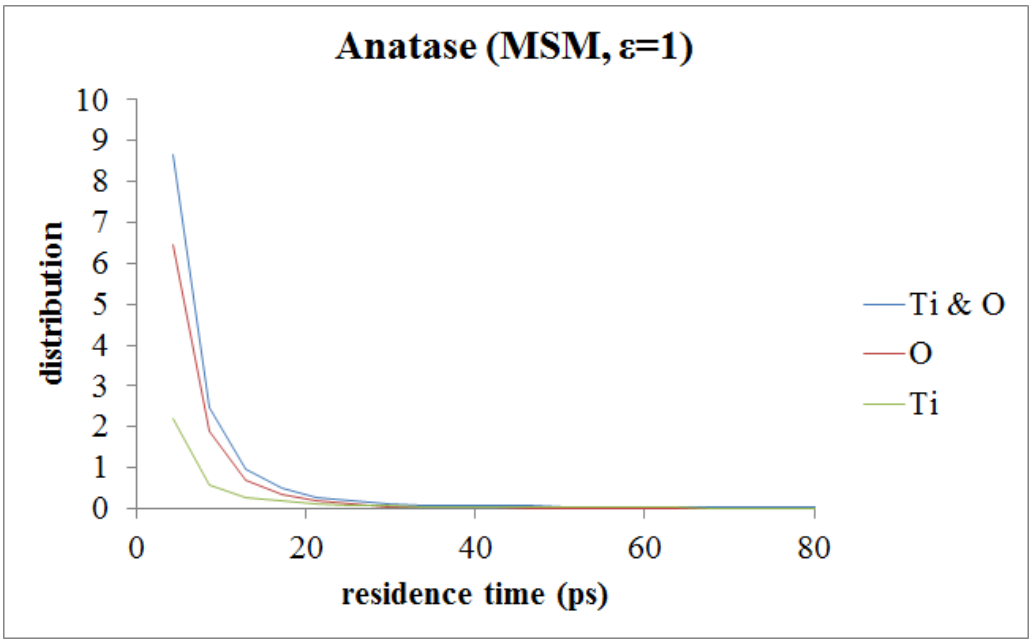

Figure 5c: Residence time distribution of water over Anatase with a dielectric constant of 1.

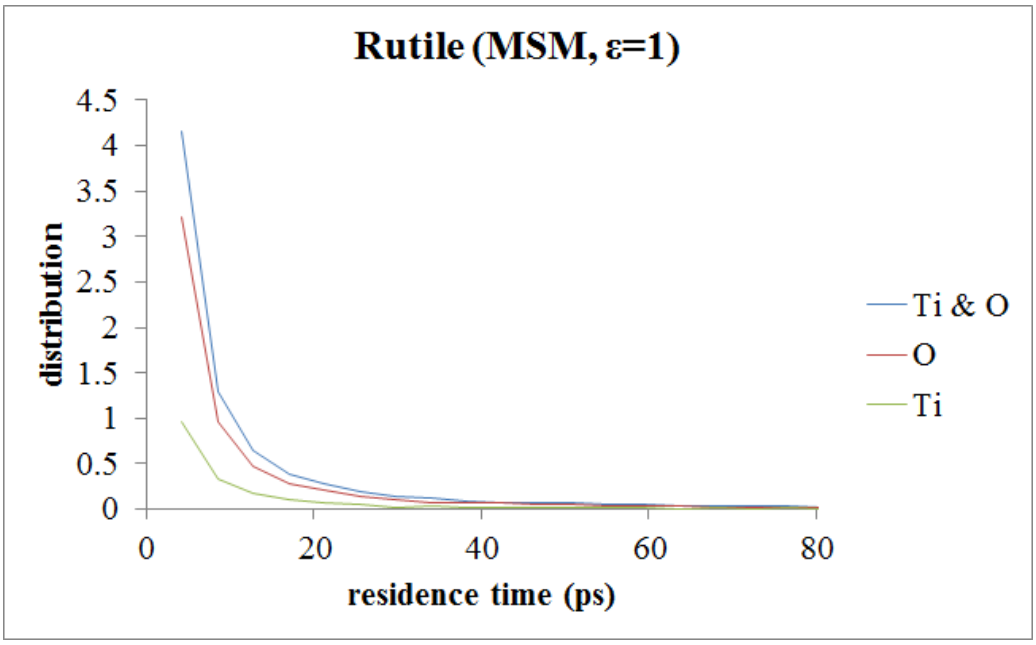

Figure 5d: Residence time distribution of water over Rutile with a dielectric constant of 1.

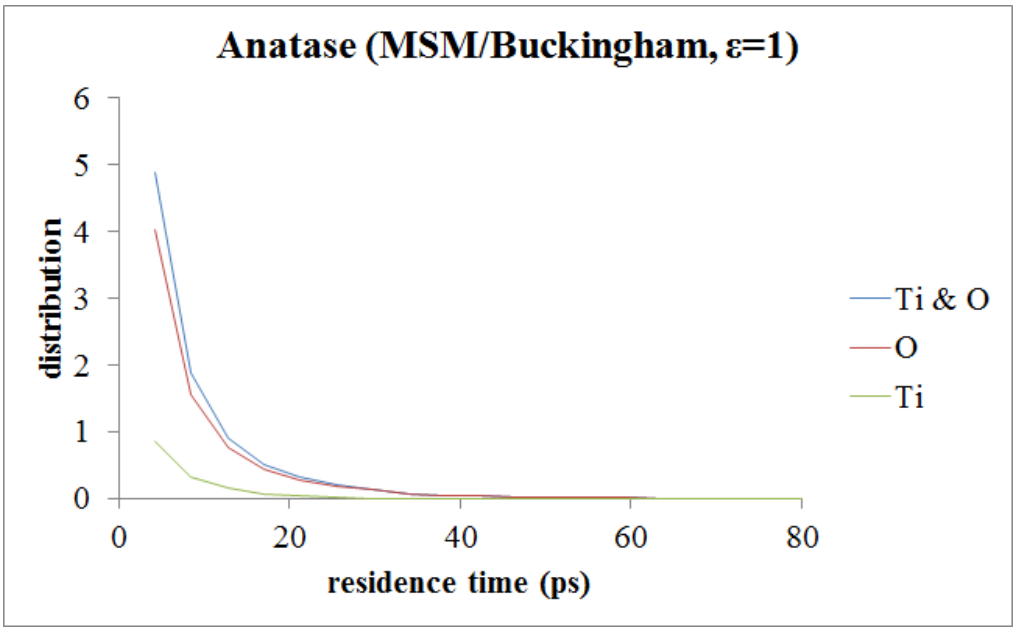

Figure 5e: Residence time distribution of water over Anatase with a dielectric constant of 1 and the Buckingham potential acting between the surface and the fluid.

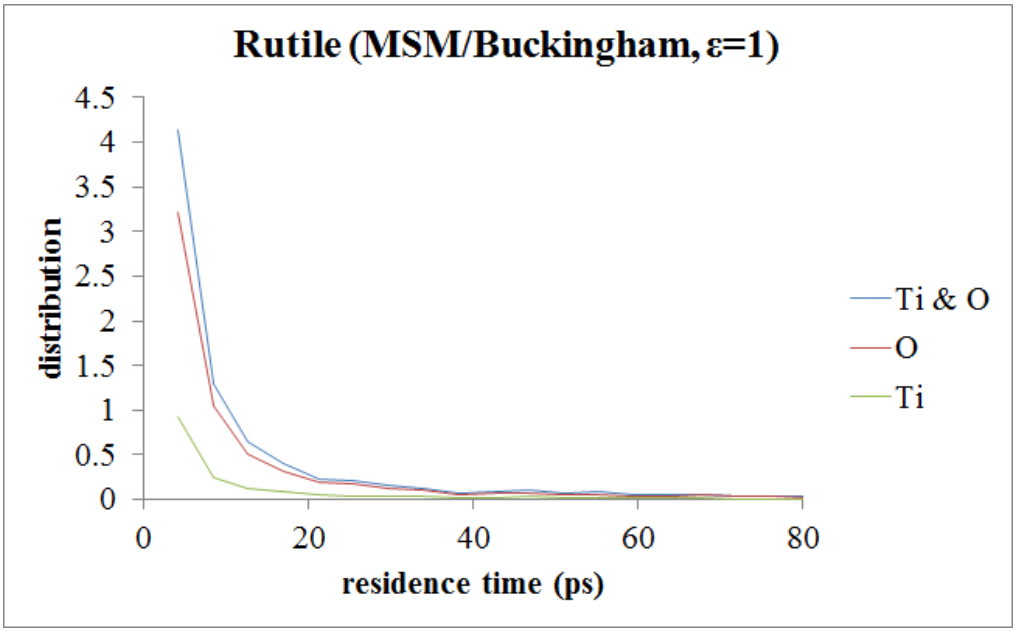

Figure 5f: Residence time distribution of water over Rutile with a dielectric constant of 1 and the Buckingham potential acting between the surface and the fluid.

4.1.5. Z-Density Profiles

To examine the adsorption of water molecules on the surfaces, we investigated the density profiles along the surface normal. The density profiles clearly demonstrate the water adsorption onto the surface to occur in layers, as shown in Figure 7. For screened Coulombic potential with a dielectric constant of 80, the profiles are similar for both anatase and rutile with the exception of the peaks occurring within ~0.3 nm from the surface. In this region, the rutile systems show two peaks whereas the anatase system shows only one peak. This observation could be attributed to the fact that the rutile surface has wider ridges with enough volume to allow water molecules to enter, adsorb and form a bilayer (see Figure 6a). This does not hold for anatase (see Figure 6b) which has much narrower ridges and insufficient inter-ridge volume for bilayered adsorption to occur. We note that the density profiles flatten out faster for the systems with a dielectric constant of 1 (at around ~0.75 nm) as compared to those with a dielectric of 80 (at around ~1.25 nm), as shown in Figure 7a. This suggests a tighter intermolecular packing in the former systems as compared to the latter which is in agreement with the RDF measurements. This also explains the similarities between the anatase and rutile surfaces at a dielectric constant given by 1. We hypothesize that the strength of the electrostatic interactions forces the layers of water molecules closest to the surface to collapse into a single layer leading to a sharp increase in the density which is more than twice of that observed in systems with a dielectric constant of 80. Our observations are in good agreement with earlier studies[8]. When the Buckingham potential is used (see Figure 7c), the rutile surface produces a packing structure very similar to corresponding results without the Buckingham potential**.** However, the anatase surface produces a peak indicating the first monolayer with no signature of the second monolayer. This could occur because

the second monolayer experiences a combined steric repulsion from the first monolayer as well as electrostatic repulsion from the highly exposed oxygen atoms on the anatase (101) surface. This combined repulsion causes the second monolayer to be "pushed" away from the surface.

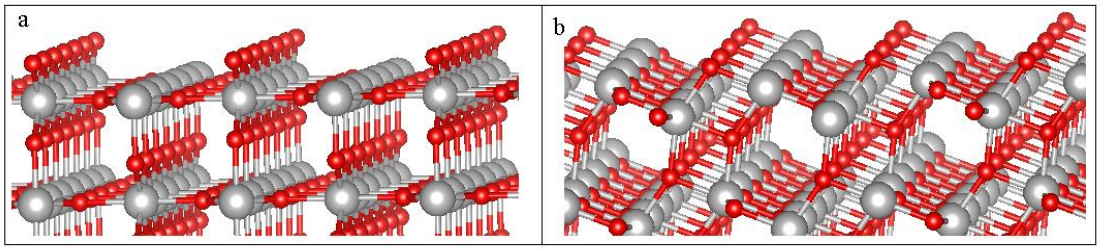

Figure 6: Ball-and-stick models for (a) Rutile 110 and (b) Anatase 101 TiO_2.

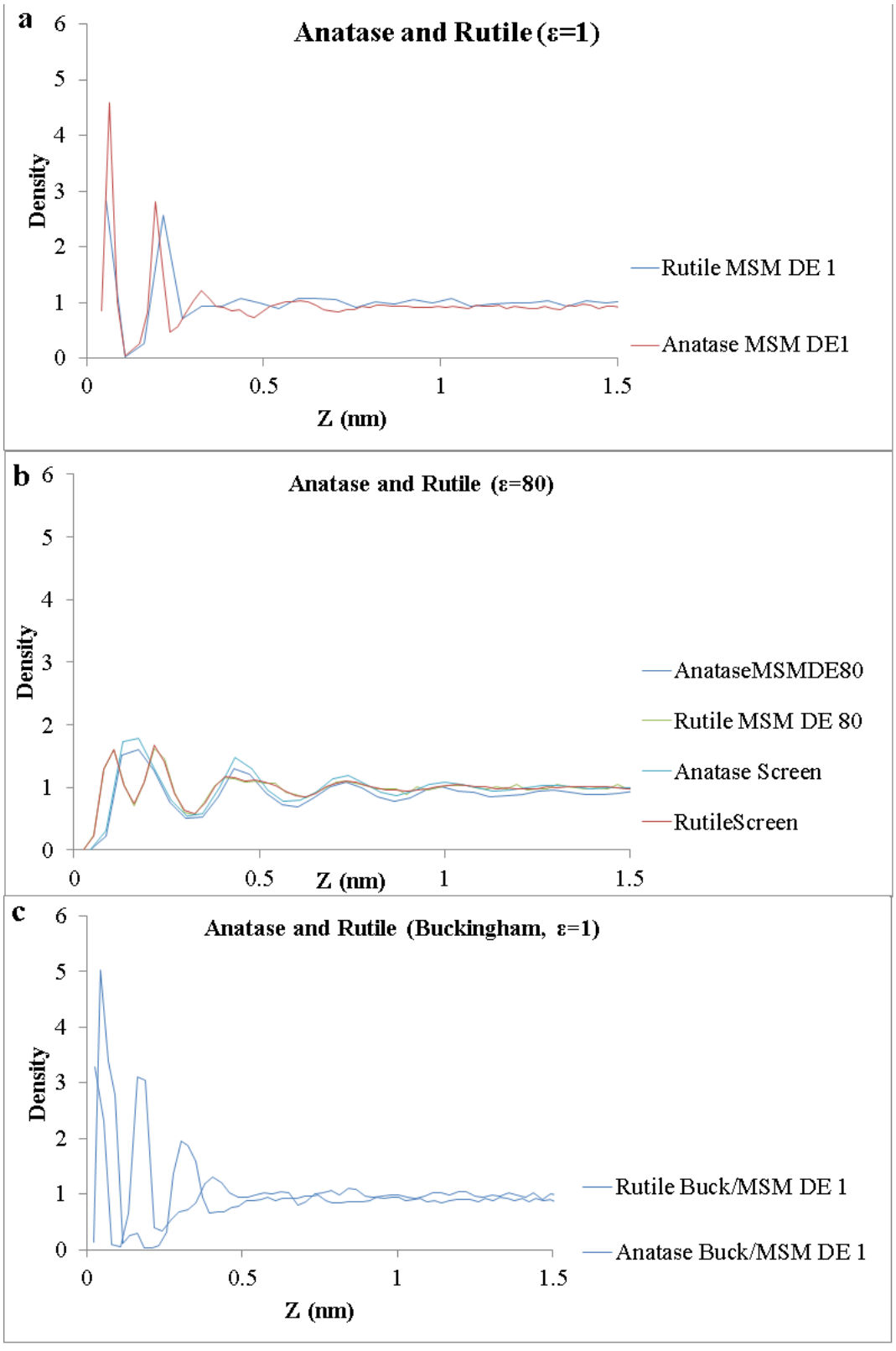

Figure 7: Density profiles along the surface normal for anatase and rutile surfaces under (a) dielectric of 1, (b) dielectric of 80, and (c) dielectric of 1 with the Buckingham Potential acting between the surface and water.

4.1.6. Adsorption Energy estimation

In addition to the density profiles, we also approximated adsorption energies. Table 3 summarizes these results. This approximation was made by first identifying the water molecules closest to the surface (the first two monolayers as indicated by the density profiles), then identifying the Titanium Dioxide surface sites closest to these water molecules, and summing and averaging the non-bonded interactions between the water and surface atoms.

Surface	**Adsorption Energy, ΔH_{ads} (eV)**		
	MSM	**MSM/Buckingham**	**Screened**
Anatase (101)	-1.08	-2.93	0.000336
Rutile (110)	-2.18	-2.74	0.000025

Table 3: Adsorption Energies

4.2 Titanium Dioxide Surfaces with Platinum Adatoms

Publication: Molecular Dynamics Study of Water over Pt/TiO_2 Surfaces, S. Mushnoori, L.Chong and M. Dutt, 2016, *Materials Today: Proceedings 3, 513 – 517.*

Collaborator: Leebyn Chong, PhD

Previous work has proposed a novel in situ method involving a polyol process with UV/O_2 photocatalytic oxidation to achieve controllable synthesis of Pt nanocrystals as small as a single Pt atom on TiO2[28]. Therefore, for the Pt/TiO_2 systems we propose a surface where Pt adatoms are uniformly distributed on rutile (110) and anatase (101) surfaces. The surface has been built such that the Pt locations reflect minimum spacing from one another to avoid overlapping interaction cutoff (Figure 8). Platinum atoms carry no charge. Two independent runs using different random seeds are used for each system.

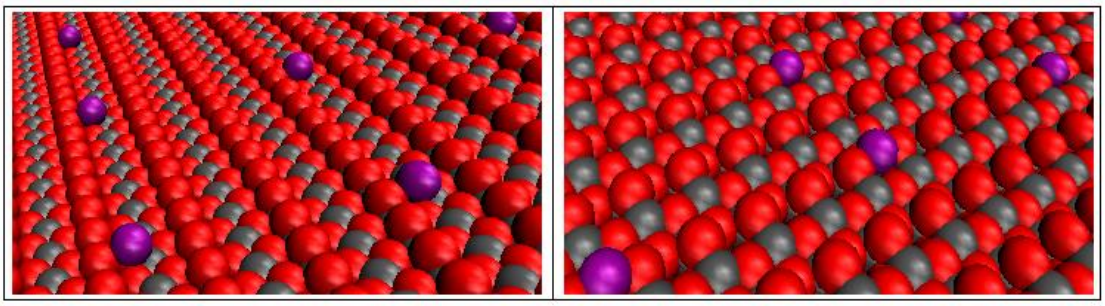

Figure 8: VMD visualizations of Rutile(110)/Pt (left) and Anatase(101)/Pt (right). Oxygen atoms represented in red, Titanium atoms in gray and Platinum atoms in Magenta.

4.2.1. Diffusion Coefficients

As validation of the model, we report the diffusion coefficient of water in bulk and water near the TiO_2 surface via mean squared displacement measurements. We observe the diffusion coefficient to be 4.733 nm^2/ns and 5.033 nm^2/ns for Pt/rutile and

Pt/anatase, respectively. This does not agree with other simulation[18] although the relative order of magnitude is maintained.

4.2.2. Radial Distribution Functions

To further verify our model, we check the radial distribution functions (RDF) of SPC/E water. Figure 9 shows our RDF for the two surfaces which agrees with the corresponding results for Lennard-Jones fluids[28]. Since we measure RDF for interior water molecules not near the surface, we expect to see very little deviations between Pt/rutile and Pt/anatase systems.

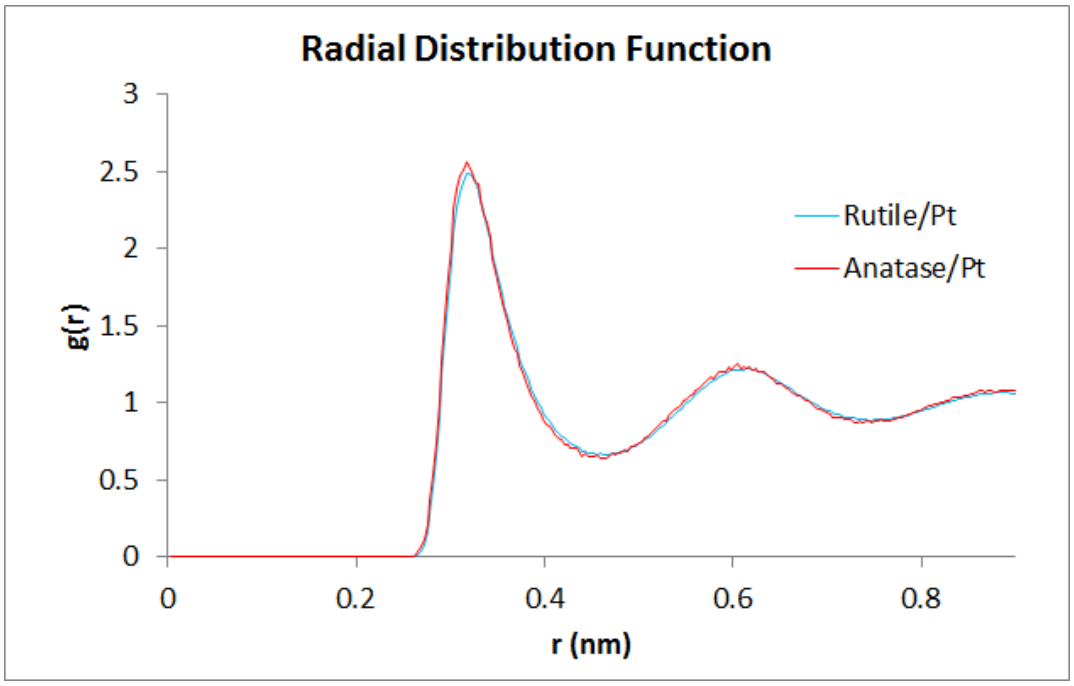

Figure 9: Radial Distribution Functions for Anatase/Pt and Rutil/Pt systems.

4.2.3. Water dipole angle distributions

We have studied the behavior of water dipoles near the surface by measuring interaction angles with respect to two different vectors: the surface normal (Fig 10a inset) and the pair vector drawn from the nearest surface atom to the center of the water molecule in question (Fig. 10b inset). Angles are defined such that an angle of 180 degrees indicates an orientation normal to the surface with the O_{water} atom pointing towards the surface, and an angle of 90 degrees implies a parallel orientation. Upon measuring the dipole angles in the bulk water system with respect to the Z-axis, we find that all angle distributions are uniform distributions, indicating that the water dipoles do not have a preferred orientation. These findings hold for the Pt/anatase as well as Pt/rutile systems. (Fig 10a, b).

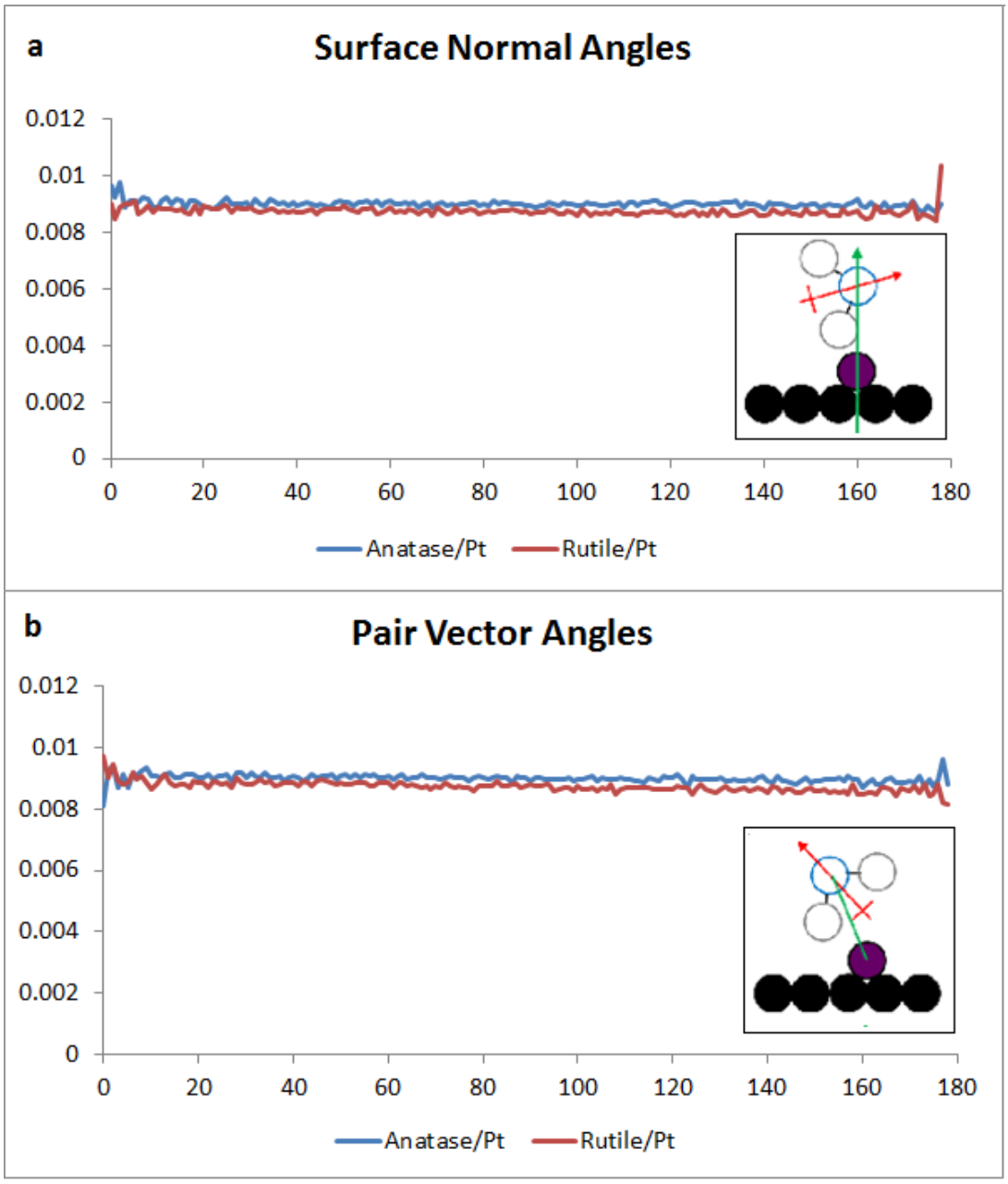

Figure 10: Angle distributions measured with respect to (a) surface normal and (b) pair vectors.

4.2.4. Residence Time Distributions

We have analyzed the residence times of water molecules in the vicinity of a given reactive site or surface atom[27]. Residence time is defined as the time spent by a water molecule inside a hemisphere of radius 1.5 σ_{OO} from a given surface atom. Residence times have been calculated with respect to $O_{surface}$ atoms only, $Ti_{surface}$ atoms only, $Pt_{surface}$ atoms only, and all surface atoms (platinum, oxygen and titanium) together. In the Pt/anatase system, water molecules that reside the longest in the vicinity of a reactive site show a residence time of roughly 15 ps, after which the distribution drops to a near-zero value (Figure 11a). The Pt/rutile system shows a much larger residence time of over 30 ps (Figure 11b). This can be attributed to the lower overall density in the Pt/anatase system as a result of the raised Pt atoms increasing the interface-liquid gap.

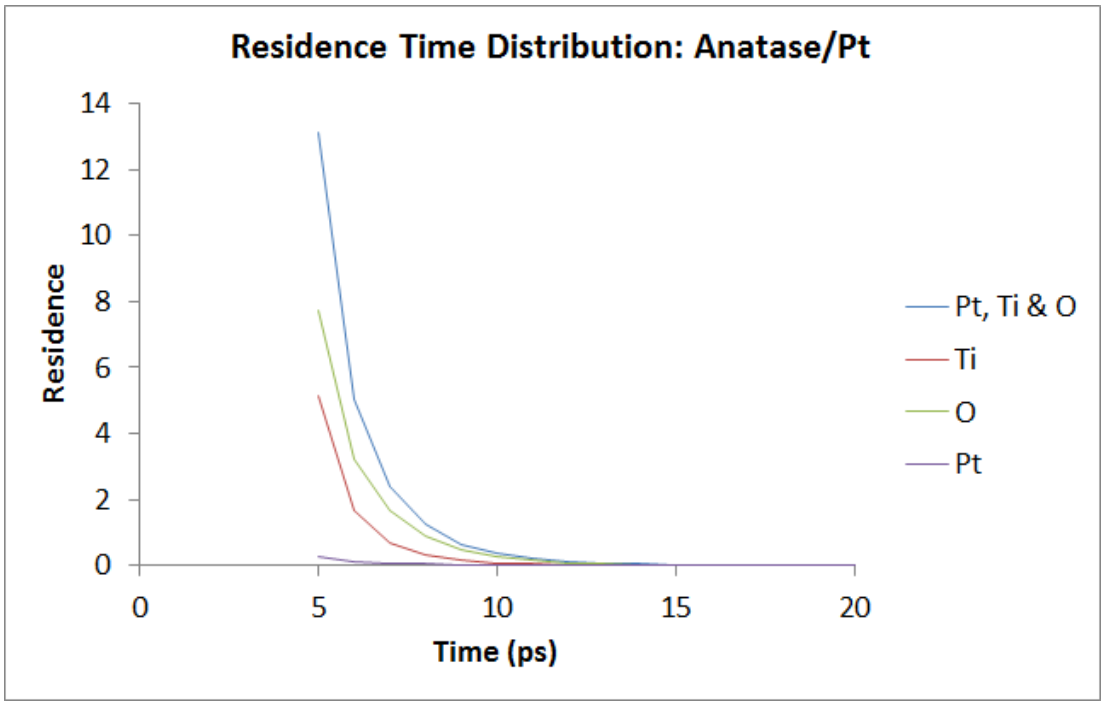

Figure 11a: Residence Time Distribution over the Anatase/Pt surface

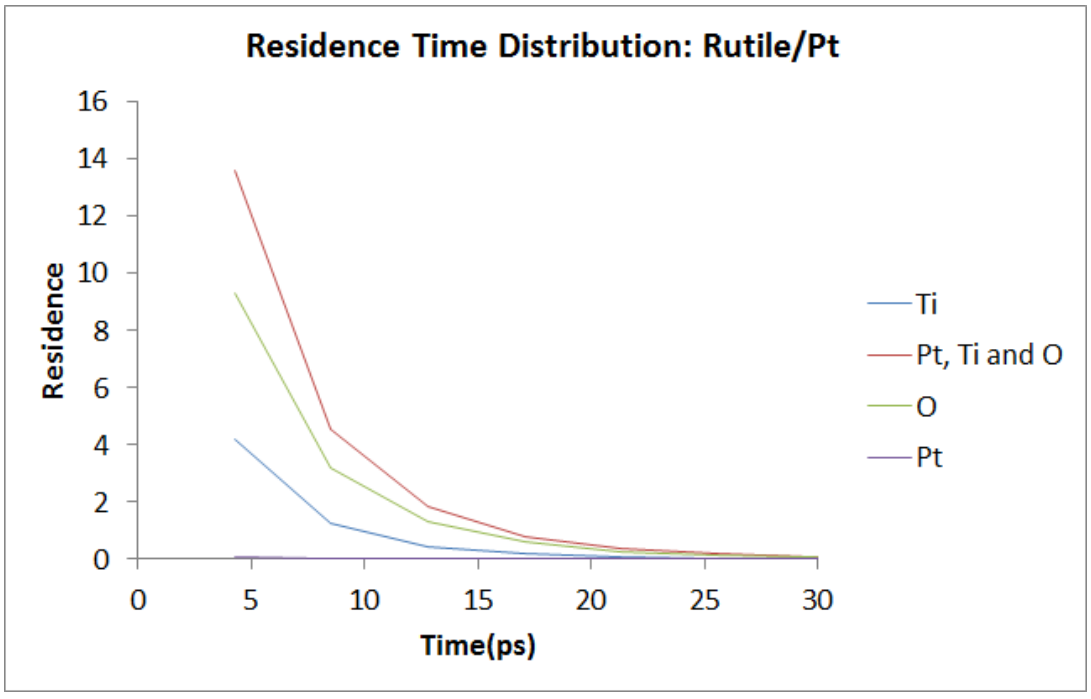

Figure 11b: Residence Time Distribution over the Rutile/Pt surface

4.2.5. Z-Density Profiles

To study the nature of adsorption on the surfaces, we investigate the density profiles along the surface normal. The density profiles clearly demonstrate the surface adsorption occurring in layers (Figure 12). The profiles are consistent with the exception of the peaks occurring within ~0.3 nm from the surface. In this region, the rutile systems show two distinct sharp peaks, whereas the anatase systems show only one. This can be attributed to the fact that the rutile surface has much deeper and wider ridges with enough volume to allow water molecules to enter. Thus, a distinct adsorption bilayer forms. However, this does not occur for anatase due to much narrower ridges and insufficient inter-ridge volume for bilayer adsorption to occur. The density profiles reach bulk density approximately 1.5 nm from the surface.

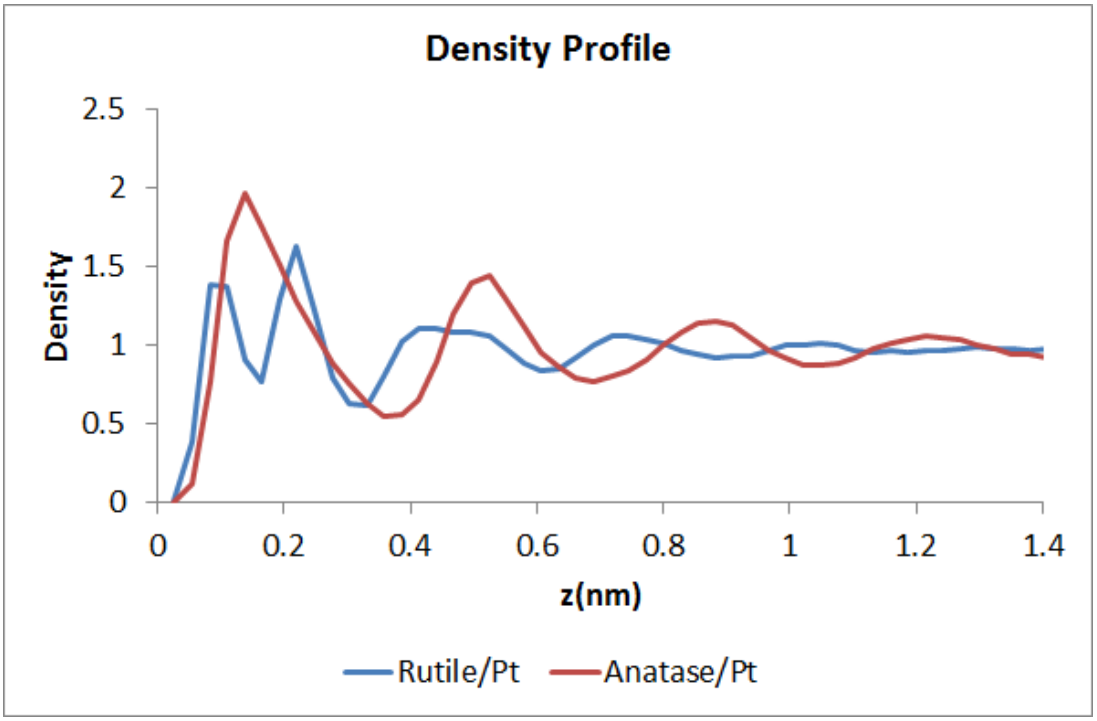

Figure 12: Density profiles over Anatase/Pt and Rutile/Pt surfaces.

5. CONCLUSIONS AND FUTURE DIRECTION

We have performed MD simulations of water on two distinct surfaces, namely anatase (101) and rutile (110) forms of titanium dioxide. Each of these systems was simulated first using the Screened Coulomb potential to model electrostatic interactions and the 6-12 Lennard Jones potential to model van der Waals interaction. The screened Coulomb potential (with the dielectric constant maintained at 80) was replaced with the Ewald Summation (dielectric constant maintained at 1). Further simulations were performed by introducing the Buckingham potential between the surfaces and the water molecules to allow for stronger electrostatic interactions between them. Our results indicate that the behavior of the system changes depending on the electrostatic model used, however this appears to be due to the difference in the dielectric constant rather than the model *per se*; when the dielectric constant was maintained at 1, the systems yielded more accurate diffusion coefficients and representation of the fluid-surface electrostatic interactions. The diffusion coefficient was found to be in agreement with the experimentally determined value and the angle distributions were consistent with dipole behavior expected near a surface consisting of oppositely charged spheres. Interestingly, comparable behaviors were observed in the diffusion coefficient, RDF, residence times and density profiles for the two values of the dielectric constant. The bulk dielectric constant, while not being able to exactly mimic bulk properties, is able to reproduce properties in the same relative order of magnitude while maintaining the electrostatic cutoff at a sufficiently small value. Furthermore, the screened Coulomb potential was applied to two additional systems: the Rutile (110) and Anatase (101) surfaces with Platinum adatoms. While the RDF and dipole angles are consistent between the two systems, differences are seen in the residence

times and density profiles, arising from differences in surface morphology and overall packing in the systems.

These results suggest the possibility of scaling to large system sizes approaching bulk-scale by using the screened Coulomb potential with a bulk dielectric constant of 80 and appropriately tweaked non-bonded interaction terms in order to more accurately reproduce properties such as diffusion coefficient. Further, there is a need to study reaction dynamics of water over titanium dioxide or other surfaces. Feasible approaches to explore this dimension include the ReaxFF force field and hybrid Molecular Dynamics/Monte Carlo simulations.

REFERENCES

1. Nagaveni, K; Sivalingam ,G.; Hegde, M.S.; Madras, G, *Photocatalytic Degradation of Organic Compounds over Combustion-Synthesized Nano-TiO2,* Environ. Sci. Technol., **2004**, *38* (5), pp 1600–1604

2. Augugliaroa, V; Bellarditaa, M; Loddoa, V; Giovanni Palmisanoa, G; Palmisanoa, L; Yurdakalb, S.; *Overview on oxidation mechanisms of organic compounds by TiO2 in heterogeneous photocatalysis.* J. Photochem. Photobiol. C, **2012**, 13,3, 224-245.

3. Jinga, J; Liu, M.;Colvinb, V.L.; Lia, W; Yu, W. W. *A Photocatalytic degradation of nitrogen-containing organic compounds over TiO2.* J. Mol. Cat. A, **2011**, 351, 17-28.

4. Zou, Z.; Ye, J.; Sayama, K.; Arakawa, H. *Direct Splitting of Water Under Visible Light Irradiation with an Oxide Semiconductor Photocatalyst.* Nature, **2001**, 414, 625-627.

5. Ellingsen, J. E. *A study on the mechanism of protein adsorption to TiO2* Biomaterials, **1991**, 12,6, 593-596.

6. Fujishima, A.; Honda, K. *Electrochemical Photolysis of Water at a Semiconductor Electrode.* Nature, **1972**, 238, 37-38.

7. Ni, M.; Leung, M.K.H.; Leung, D.Y.C.; Sumathy, K. *A Review and Recent Developments in Photocatalytic Water-Splitting Using TiO2 for Hydrogen Production.* Renew. Sust. Energ. Rev., **2007**, 11, 401-425.

8. Kavathekar, R.S.; Dev, P.; English, N.J.; MacElroy, J.M.D. *Molecular Dynamics Study of Water in Contact with the TiO2 Rutile-110, 100, 101, 001 and Anatase-101, 001 Surface.* Mol. Phys., **2011**, 109, 1649-1656.

9. Kavathekar, R. S.; English, N. J.; MacElroy, J. M. D. *Study of Translational, Librational and Intra-Molecular Motion of Adsorbed Liquid Water Monolayers at Various TiO2 Interfaces.* Mol. Phys., **2011**, 109, 2645-2654.

10. Kavathekar, R. S.; English, N. J; MacElroy, J. M. D. *Spatial Distribution of Adsorbed Water Layers at the TiO2 Rutile and Anatase Interfaces.* Chem. Phys. Lett., **2012**, 554, 102-106.

11. English, N. J. *Dynamical Properties of Physically Adsorbed Water Molecules at the TiO2 Rutile-(1 1 0) Surface.* Chem. Phys. Lett., **2013**, 583, 125-130.

12. Alder, B. J.; Wainwright, T. E. *Studies in Molecular Dynamics. I. General Method.* J. Chem. Phys., **1959**, 31, 459-466.

13. Allen, M. P.; Tildesley, D. J. *Computer Simulation of Liquids.* Oxford : Clarendon Press, **1987**.

14. Frenkel, D.; Smit, B. *Understanding Molecular Simulation: From Algorithms to Applications.* 2nd. San Diego : Academic Press, **2002**.

15. Plimpton, S. *Fast Parallel Algorithm for Short-Range Molecular Dynamics.* J. Comput. Phys., **1995**, 117, 1-19.

16. Debye, P.; Huckel, E. *The Theory of Electrolytes. I. Lowering of Freezing Point and Related Phenomena.* Physikalische Zeitschrift, **1923**, 24, 185-206.

17. Hardy, D.J.; Wu, Z.; Phillips, J.C.; Stone, J.E.; Skeel, R.D.; Schulten, K. *Multilevel Summation Method for Electrostatic Force Evaluation.* J. Chem. Theory Comput., **2015**, 11, 766-779.

18. Mark, P.; Nilsson, L. *Structure and Dynamics of TIP3P, SPC, and SPC/E Water Models at 298 K.* J. Phys. Chem. A, **2001**, 105, 9954-9960.

19. Wasserman, E.; Wood, B.; Brodhol, J. *The Static Dielectric Constant of Water at Pressures up to 20 kbar and Temperatures to 1273 K: Experiment, Simulations, and Emperical Equations.* Geochim. Cosmochim. Ac., **1995**, 59, 1-6.

20. Berendsen, H. J. C.; Grigera, J. R.; Straatsma, T. P. *The Missing Term in Effective Pair Potentials.* J. Phys. Chem., **1987**, 91, 6269-6271.

21. Bandura, A. V.; Kubicki, J. D. *Derivation of Force Field Parameters for TiO2-H2O Systems from Ab Initio Calculations.* J. Phys. Chem. B, **2003**, 107, 11072-11081.

22. Zhao, W. N.; Liu, Z. P. *Mechanism and Active Site of Photocatalytc Water Splitting on Titania in Aqueous Surroundings.* Chem. Sci., **2014**, 5, 2256-2264.

23. Park, J. H.; Aluru, N. R. *Temperature-Dependent Wettability on a Titanium Dioxide Surface.* Mol. Simulat., **2009**, 35, 31-37.

24. Schneider, T.; Stoll, E. P. *Molecular-Dynamics Study of a Three-Dimensional One-Component Model for Distortive Phase Transitions.* Phys. Rev. B, **1978**, 17, 1302-1322.

25. Holz., M.; Heil, S. R.; Sacco, A. *Temperature-dependent Self-diffusion Coefficients of Water and Six Selected Molecular Liquids for Calibration in Accurate 1H NMR PFG Measurements.* Phys. Chem. Chem. Phys., **2000**, 2, 4740-4742.

26. Morsali, A.; Goharshadi, E.K.; Mansoori, G.A. *An Accurate Expression for Radial Distribution Function of the Lennard-Jones fluid.*, Chem. Phys., **2005**, 310, 11-15.

27. Chong, L; Dutt, M. *Computer simulations of fluid flow over catalytic surfaces for water splitting.* Appl. Surf. Sci., **2014**, 323, 96-104.

28. Jiang, Z.; Guo, H.; Jiang, Z.; Chen, G.; Xia, L.; Shangguan, W.; Wu, X. *In Situ Controllable Synthesis Platinum Nanocrystals on TiO2 by Novel Polyol-Process Combined with Light Induced Photocatalysis Oxidation*. Chem. Commun. **2012**, 48, 9598-9600.

ACKNOWLEDGEMENT OF PREVIOUS PUBLICATIONS

1. A Computational Study of the Organization and Dynamics of Water on Anatase (101) and Rutile (110) Titania Surfaces: The Effect of Electrostatic Models, S. Mushnoori, L.Chong and M. Dutt, 2016, Submitted.

2. Molecular Dynamics Study of Water over Pt/TiO_2 Surfaces, S. Mushnoori, L.Chong and M. Dutt, 2016, Materials Today: Proceedings 3, 513 – 517.